Journal of Cereal Science 52 (2010) 136–142

Contents lists available at ScienceDirect

Journal of Cereal Science

journal homepage: www.elsevier.com/locate/jcs

Field emission scanning electron and atomic force microscopy, and Raman and X-ray photoelectron spectroscopy characterization of near-isogenic soft and hard wheat kernels and corresponding flours

L. Scudiero [a], Craig F. Morris [b,*]

[a] Chemistry Department and Materials Science and Engineering Program, Fulmer 261A, Washington State University, Pullman, WA 99164, USA
[b] USDA-ARS Western Wheat Quality Laboratory, E-202 Food Science & Human Nutrition Facility East, Washington State University, Pullman, WA 99164-6394, USA

ARTICLE INFO

Article history:
Received 30 December 2009
Received in revised form
19 March 2010
Accepted 15 April 2010

Keywords:
Wheat
Kernel
Texture
Microscopy

ABSTRACT

Secondary field emission scanning electron microscopy (FE SEM), atomic force microscopy (AFM), Raman spectroscopy and X-ray photoelectron spectroscopy (XPS) were used to investigate native near-isogenic soft and hard wheat kernels and their roller milled flours. FE SEM images of flat-polished interior endosperm indicated distinct differences between soft and hard wheats with less internal continuity in the soft wheat, whereas individual starch granules were much less evident in the hard kernel due to a more continuous matrix. AFM images revealed two different microstructures. The interior of the hard kernel had a granular texture with distinct individual spheroid features of 10–50 nm while the images obtained for the soft kernel revealed less distinct small grains and more larger features, possibly microstructural features of starch granules. Raman spectra resolved identical distinct frequencies for both kernel types with slightly different intensities between types. Finally, the chemical surface compositions of flour for these two types of kernels obtained by XPS provided subtle insight into the differences between soft and hard wheat kernels. These combined advanced microscopic and spectroscopic analyses provide additional insight into the differences between the soft and hard wheat kernels.

Published by Elsevier Ltd.

1. Introduction

Kernel texture ("hardness") is a fundamental and over-arching property of wheat (*Triticum* spp.) grain. In hexaploid wheat (*Triticum aestivum*), two major texture classes are recognized and are referred to simply as 'soft' and 'hard' ('floury' and 'vitreous' kernels may exist in either texture class, Morris, 2002). This distinction is included in most marketing systems around the world as it influences many aspects of milling, flour particle size, starch damage, processing and food product properties. The genetic basis for the difference between soft and hard wheat is now well known. Soft texture results from the presence of puroindoline a and puroindoline b genes together in a particular primary structure (Morris, 2002; Bhave and Morris, 2008a, b). If genetic mutation alters the primary structure or interferes with expression, hard texture results. The mechanism by which puroindolines soften kernels is essentially unknown. What is known is that soft and hard wheat endosperms differ in their fundamental material properties as evidenced by failure stress, failure strain and failure energy (Morris et al., 2008a, b). These differences are ascribed to differences in adhesion between cell constituents, namely starch granules and protein matrix, and possibly cell walls. Currently, powerful microscopic and spectroscopic techniques such as atomic force microscopy, Raman and X-ray photoelectron spectroscopy (XPS) are available to study this important phenomenon. The examination of endosperm from soft and hard wheat kernels with these techniques has not heretofore been attempted on native kernels and flours in the absence of special treatments such as sputter coating for FE SEM, UV/ozone treatment, soaking in water or mixing with other ingredients. A notable feature of the present work is the use of genetically near-isogenic lines.

Atomic force microscopy (AFM) is a powerful tool to characterize flat surfaces without special preparation from the micrometer to nanometer scale. Yet, until recently it has not been used extensively in food science research. Its utilization has been growing rapidly, however, with studies of rheology in food biopolymers (Morris et al., 2001), the surface of starch granules of barley (Baker et al., 2001), maize (Juszczak et al., 2003; Ohtani et al., 2000) and pea (Ridout et al., 2006). It has also been used to image

* Corresponding author. Tel.: +1 509 335 4062; fax: +1 509 335 8573.
E-mail addresses: scudiero@wsu.edu (L. Scudiero), morrisc@wsu.edu (C.F. Morris).

0733-5210/$ – see front matter Published by Elsevier Ltd.
doi:10.1016/j.jcs.2010.04.005

bacteria (Bolshakova et al., 2004) and the skin of peaches (Yang et al., 2004). Its basic principle is explained in depth in the literature (Binnig et al., 1986; Dufrene, 2001; Yang and Shao, 1995). We used the AFM in this work to analyze the endosperm of genetically near-isogenic soft and hard wheat kernels. The surface morphology contributes insight as to the differences between these two kernel texture types, and therefore information as to the manifestations of puroindolines and kernel texture.

Spectroscopic techniques such as Raman and X-ray photoelectron spectroscopy (XPS) can be used to examine differences between soft and hard wheat samples and allow quantification of constituents. The use of Raman spectroscopy in food science analysis has increased dramatically during the last two decades. Studies on carbohydrates (Bulkin et al., 1987; Arboleda and Loppnow, 2000; Synytsya et al., 2003; Fechner et al., 2005), lipids (Strehle et al., 2006), changes in protein–protein interactions (Howell et al., 1999), protein–lipid interactions (Meng et al., 2005), and protein–carbohydrate interactions (Alizadeh-Pasdar et al., 2002) in food systems have been performed. Characteristic frequencies of chemical functional groups and their intensities can be determined by Raman spectroscopy. Quantitative surface chemical composition and chemical energy shift of the composing elements of most materials can be obtained by X-ray photoelectron spectroscopy (XPS). The energy shift translates to chemical bonding information.

Spectroscopic techniques have been widely used by others (Neethirajan et al., 2008; Rouxhet et al., 2008; Barton and Himmelsbach, 2002) For instance, near-infrared spectroscopy (NIRS) is routinely used for quality testing of crossbred materials from wheat breading programs (Osborne, 2001) and on-line monitoring of starch damage, moisture content, and protein (Barron and Rouau, 2008). Its utilization requires, however, a rigorous calibration against reference samples of grains and flours. Piot et al. (2000, 2001) examined differences in soft and hard wheat grains from different varieties. The specific varieties were not identified, but observations related to interstitial protein between starch granules and changes in arabinoxylan content could not be conclusively associated with kernel texture (i.e., results were confounded with variety).

In this study, we applied advanced microscopic and spectroscopic techniques to investigate differences in genetically near-isogenic soft and hard wheat kernels and their corresponding roller milled flour with no special treatments (tissue fixation, UV/ozone treated, sputter coating, soaking in water and/or mixed with other ingredients).

2. Experimental

Wheat kernels were from the near-isogenic soft and hard wheat lines developed in the spring cultivar Alpowa (Morris and King, 2008). Flours of each were prepared using standard milling operations and a modified Quadrumat (C.W. Brabender Instruments, Inc., South Hackensack, NJ) laboratory roller mill (Jeffers and Rubenthaler, 1977). Protein content was obtained using combustion nitrogen determination (Dumas, Leco FP-428, Leco Corp., St. Joseph, MI) (Approved Method 46-30, AACCI 2000), and a conversion factor of 5.7. Moisture content was determined using thermogravimetric analysis (Leco TGA-601).

Prior to imaging, the kernels were glued to metallic plucks with cyanoacrylate ('superglue') and polished in three steps with Fandeli coated abrasive (SiC) starting at 600 grading followed by 1200 and 1500 grading. The kernel faces were then blown gently with compressed air (Gust Easy Duster, Stoner, Quarryville, PA) to remove residual flour produced by the polishing.

One sample of each kernel type were imaged by secondary field emission scanning electron microscopy (FE SEM) without sputter coating on a Quanta 200F microscope (FEI Co., Hillsboro, OR) under the conditions and magnifications shown on each figure (see Fig. 1).

Interior endosperm microstructure information was obtained on the same SEM samples and on at least three more different kernels of each type from the same pool of wheat by atomic force microscopy (AFM). A Nanoscope III (Veeco, Santa Barbara, CA) was used in contact mode to produce the topographic images. An ultrasharp Si cantilever with radius of curvature of 10 nm and spring constant of 2 N/m was used to generate the images. A scanning probe imaging process, SPIP, commercial software (ImageMetrology A/S, Horsholm, Denmark) was used to process the raw images. Planefit and median filtering 5×5 were the only processings applied to the images unless specified otherwise in the captions. An Advantage 200A Raman spectrometer (DeltaNu Inc., Laramie, WY) with 5 mW power laser, 632 nm light and 1800 lines/mm was used to record Raman spectra of wheat flour obtained from soft and hard wheat. This technique provided only a relative comparison (presence or absence of bands and intensity of bands) between the two types of wheat due to the limited resolution of this spectrometer (10 cm^{-1}). Raman spectroscopy was used on five different samples from the same flour. The spectra are the average of 1000 scans. An integration time of 25 s was used. The real-time baseline subtraction was applied to remove fluorescence from the spectra. In addition, a 51 points Savitsky-Golay smoothing filtering was applied to the spectra to enhance the bands and reduce the noise level.

The XPS analysis was performed with an Axis-165 (Kratos Analytical Inc. Manchester, UK). Achromatic X-ray radiation of 1253.6 eV (MgKα) was utilized as the XPS excitation source for acquiring all photoelectron spectra. The binding energies were calibrated against the Au $4f_{7/2}$ peak taken to be located at 84.19 eV and Ag $3d_{5/2}$ peak at 368.46 eV. The base pressure of the analyzing chamber was 7×10^{-10} Torr. The curve fitting of the O 1*s* and C 1*s* data was performed with CasaXPS commercial software (Casa Software Ltd., Teignmouth, Devon, UK) with full width half maximum (FWHM) of about 1.8 eV and a Gaussian–Lorentzian line shape (GL30) for all components of the same peak. The flour samples were pressed against 99.99% pure indium flattened shots (Alfa Aesar) prior to placing the samples in the vacuum chamber. The spectra of nitrogen, oxygen and carbon were shifted by the same energy to correct for a small static charging to set C–C or C–H component of C1s at binding energy (BE = 284.6 eV).

3. Results and discussion

3.1. FE SEM images

Field emission (FE) SEM (without sputter coating) was used first to examine the native polished exposed interior endosperm from soft and hard near-isogenic wheat kernels. Fig. 1A and B shows the general preparation of soft and hard kernels, respectively, for AFM. Kernels were polished to expose the central endosperm. At this magnification, only the general morphology of the caryopses is discernible. Fig. 1C and D provide approximately 50-fold greater magnification. At this resolution, discrete features are visible as well as some topography. In the soft wheat endosperm, features were visible that would likely be large A-type starch granules and smaller B-type starch granules. A continuous protein matrix was not present and the polished surface was irregular with a significant amount of cross-sectional area below the polishing plane. The hard wheat endosperm (Fig. 1D) in contrast did not reveal easily discernable A-type starch granules, although discontinuities of approximately the correct size (ca. 20 μm) were present. These discontinuities were often bright due to charging of the edges of these features. Smaller bodies that could correspond to B-type granules were present.

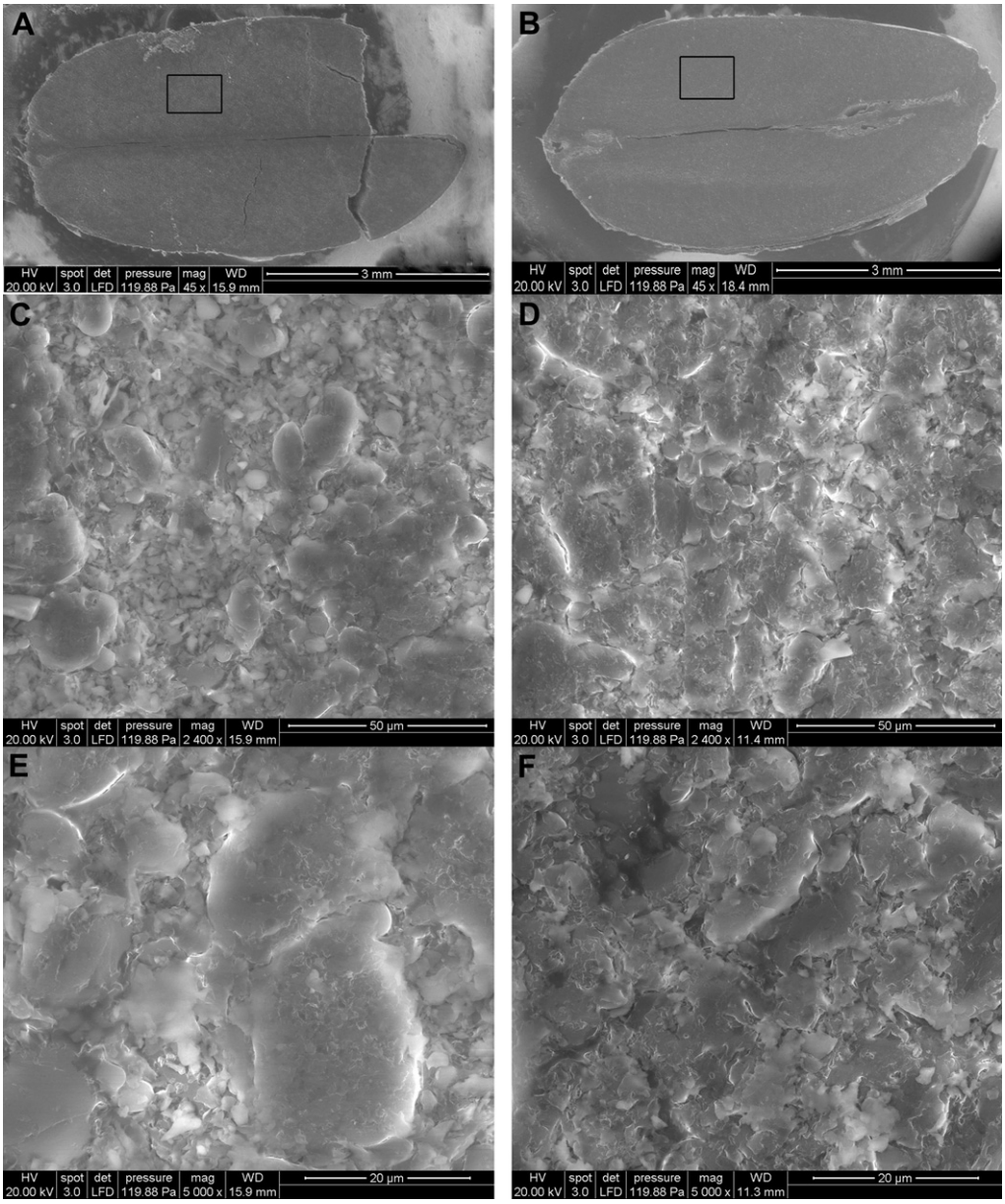

Fig. 1. FE SEM of the intact soft (A, C, E) and hard (B, D, F) near-isogenic wheat kernels showing the exposed interior polished surface. These specimens were used for FE SEM images of greater resolution (C–F). The box indicates the generalized area that AFM images were derived (Fig. 2). FE SEM conditions, magnification and scale bar appear in the bottom of the image.

However, by-and-large, much of the cross-sectional surface appeared to lie within the polishing plane and was much more continuous. Upon further magnification (Fig. 1E and F), further topography was revealed. In the soft endosperm, what would be construed as an A-type granule was seen to be polished through its interior and a slightly rough, almost 'flaked' appearance was present at the polished plane. Charging of these 'micro' edges enhanced the visibility of these features. Other features were present on the scale of B-type starch granules and these lay below the polishing plane. The hard wheat endosperm at the greatest magnification (Fig. 1F) showed considerable topography, even though much of the cross-sectional area appeared to lie near the polishing plane. Fewer discrete features were observed with some areas fairly smooth and others with noticeable edges that were enhanced due to charging. These FE SEM images indicated distinct differences between near-isogenic soft and hard wheat endosperm, and provided insight as to the utility of the polishing procedure for AFM analysis.

3.2. AFM images

The microstructure of any "flat" surface is easily analyzed by atomic force microscopy (AFM). We used the technique to obtain the surface morphology of exposed, polished endosperm from soft and hard wheat kernels under ambient conditions. Fig. 2 shows 100×100 µm AFM images of both types of kernels. Fig. 2A shows the AFM image obtained for the soft wheat kernel endosperm. Clusters formed by starch granules dominate the image with fewer distinct, individual smaller features. The average roughness is 1739 nm and the surface area ratio (surface area/scanning area) was about 2.2. The hard kernel endosperm surface morphology (Fig. 2B) was noticeably different. AFM revealed a granular texture with larger features ranging in size from 10 to 50 nm with an average roughness of 2053 nm. The surface area ratio was about 3.8. This difference in surface area ratio between soft and hard wheat endosperm could be explained by a lower density of starch in the

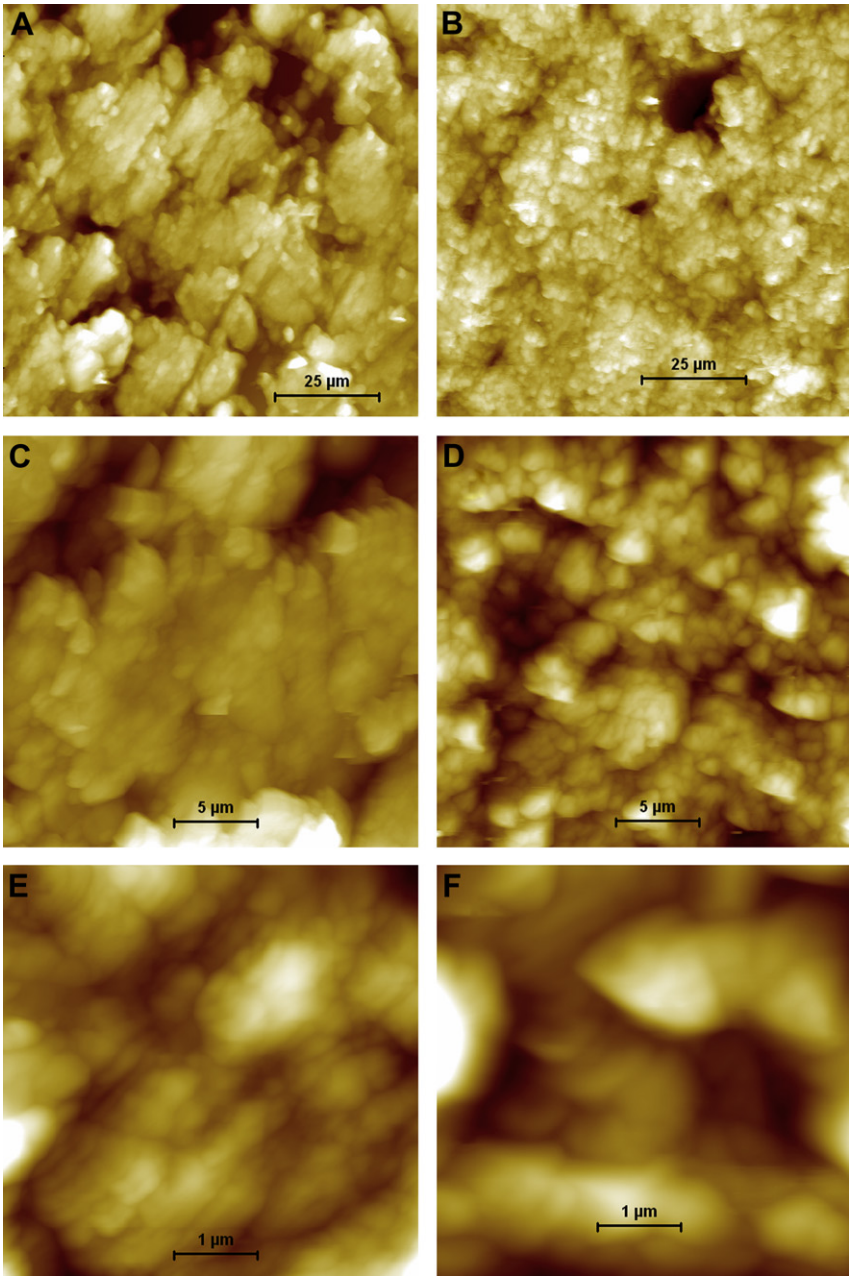

Fig. 2. AFM images acquired in height mode of intact soft (A, C, E) and hard (B, D, F) near-isogenic wheat interior polished endosperm; 100 × 100 μm (A and B); 25 × 25 μm (C and D); 5 × 5 μm (E and F). These images were acquired at the generalized (boxed) area indicated in Figs. 2 and 1, respectively.

case of the soft wheat kernel, but may also be a direct result of the fundamental differences between adhesion/microscopic structure and composition of soft and hard kernels. Fig. 2C and D are higher resolution AFM images (25 × 25, and 5 × 5 μm, respectively). These AFM micrographs support the difference in microstructure between the two types of wheat kernel endosperm seen in the larger-scale images. For instance, distinct clusters are easily seen in Fig. 2E. The clusters are 1–3 μm across with smaller features on the order of 100–500 nm. These very small features are not evident in the hard endosperm (Fig. 2F) in which distinct individual features of about 1 μm were present. Although the morphological/topographical differences in microstructure between these two kernel types were relatively small, the AFM was able to image it. It should be noted that these specimens were physically disturbed, i.e. polished, and that physical–chemical differences at a microscopic level could respond differently to the polishing process.

3.3. Raman spectra

Peaks in Raman spectroscopy can be related to specific chemical functional groups and their positions are sensitive to the local environment. Photons of light interact with the sample to produce scattered radiation of different wavelengths; the difference between incident and scattered wavelengths is the Raman shift and is expressed in wavenumbers (cm^{-1}). In this study, we measured several distinct broad bands in the regions of 280 cm^{-1}, 480–580 cm^{-1}, 760 cm^{-1}, 940 cm^{-1}, 1130–1390 cm^{-1}, 1460 cm^{-1} and 1660 cm^{-1} as seen in Fig. 3A. A weak band was also measured at 2905 cm^{-1} (Fig. 3B). The spectra shown in the figures were corrected for fluorescence emission and smoothed using the Savitzky–Golay algorithm (local second order polynomial regression; filtering). Note that the main concern in this study was to identify differences between soft and hard wheat flour of the Alpowa near-isogenic lines.

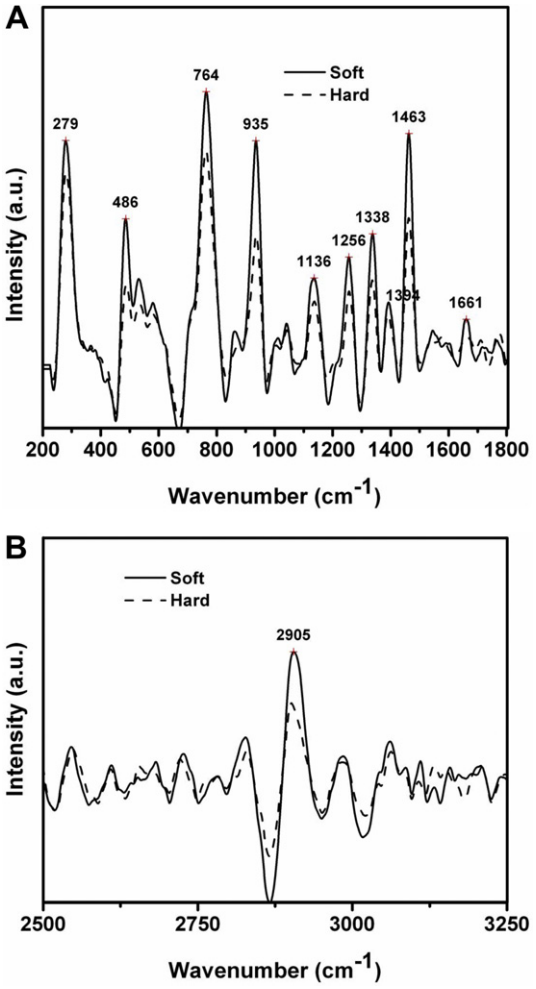

Fig. 3. Raman spectra obtained on near-isogenic soft and hard wheats flours; (A) 200–1800 cm^{-1}, (B) 2500–3250 cm^{-1}. A real-time baseline subtraction and 51 points smoothing S–G filtering was apply to the spectra. Note the difference in intensity of the bands between soft and hard flours.

Although the same Raman shifts were measured for both types of flour, the intensity of the bands differed. A tentative assignment of these bands is summarized in Table 1 that follows the work of Piot et al. (2000, 2001) and Barron and Rouau (2008) on wheat grain, and of Sandras et al. (2009) on puroindoline a. The intensity difference between the two types of flour cannot be easily explained. However, relative intensity ratios of bands in the 400–600 cm^{-1} and 1020–1650 cm^{-1} could be used to assess arabino-to-xylan substitution and/or phenolic acid contents as observed by Barron and Rouau (2008). For instance, the band at 486 cm^{-1} compared with 579 cm^{-1} for soft and hard flour is different. A ratio of 0.34 was estimated for the soft flour compared to 0.57 for hard flour. Similarly the ratio of the weak band around 1660 cm^{-1} to the band at about 1136 cm^{-1} gives a relative content of phenolic acid. Values of 0.25 and 0.16 were obtained for soft and hard, respectively. Although it is not possible to explain why a wheat kernel is soft or hard based only on Raman spectroscopy, the technique provided some insight into the chemical functional groups. This is in good agreement with the results of Barton and Himmelsbach (2002) who applied vibrational spectroscopy to analyze wheat and concluded that the spectral difference between soft and hard was very small. In conclusion, the broad Raman bands measured at ~500 cm^{-1}, ~750 cm^{-1}, ~1000 cm^{-1}, 1100–1300 cm^{-1} and ~1450 cm^{-1} are consistent with data found in the literature (Barton and Himmelsbach, 2002; Centre for Advanced Microscopy (CfAM), 2006; Cao et al., 2006; Liu et al., 2009) for wheat flour. For instance, bands in the region of 480–650 cm^{-1} are attributed to the distribution of starch (Celedon and Aguilera, 2002; Baranska et al., 2005), bands in the region of 650–800 cm^{-1} to C–H bending, in the region of 900–1150 cm^{-1} are associated with C–C and C–O stretching (carbohydrates) (Centre for Advanced Microscopy (CfAM), 2006) and in the region of 1400–1500 cm^{-1} to the C–H bending and C=O stretch in COO (proteins) (Dhanasettakorn, 2008). The weak band at about 2905 cm^{-1} was assigned to a C–H stretch and was also observed by Barton and Himmelsbach (2002). In conclusion, Raman spectroscopy can point towards differences in flours, but a narrow and specific interpretation of the bands in these complex systems remains equivocal.

Table 1
Tentative assignment of Raman bands in near-isogenic soft and hard wheat flours.

Raman shift (cm^{-1})	Assignment
279	(C–C), bending
486–580 (m)	(S–S),[a] stretching
764 (s)	W18 Trp[a]
935 (s)	(C–C),[a] arabinoxylan,[b] stretching
1136 (w)	W13 Trp,[a] arabinoxylan[b]
1256 (w)	(Amide III, W11 Trp),[a] C–C stretching[b]
1338 (m)	W7 Trp,[a] COC and CO[b]
1463 (s)	(CH_2 or CH_3),[a] CH and COH bending[b]
1661	(Phenolic ring/Trp),[a] Phenolic ring[b]
2905	(symmetricCH_2-asymetricCH_3[a]),[a] bending

[a] Sandras et al. (2009).
[b] Barron and Rouau (2008).

3.4. XPS spectra

X-ray photoelectron spectroscopy was used to differentiate the surface chemical composition of the two types of flours. This technique uses soft X-rays to eject electrons from the surface of a sample. The energy at which the electrons are ejected is characteristic of an element (with the exception of hydrogen) and the area under the peak generated is used to obtain quantitative information expressed in relative atomic concentration percentage (At%). Table 2 summarizes the relative atomic concentration of carbon, nitrogen and oxygen measured for both wheat flours. Note that in this work we were unable to detect sulfur in our samples due to its very low content and high noise level in our XPS spectra. The energy shift measured with XPS was used to obtain chemical bonding information as seen in Fig. 4. The XPS spectra of N 1*s* (Fig. 4A) display a single peak at ~399.7 eV characteristic of amide or amine for both soft and hard wheat flours. In contrast, the XPS

Table 2
Surface atomic concentration (At%) of carbon, nitrogen and oxygen of wheat flours.

Wheat kernel	Element	Binding energy (eV)	At%
Soft	O	531.3	13.9
		532.6	3.2
		534.3	2.7
	N	399.7	3.0
	C	284.6	52.2
		286.5	16.8
		288.2	8.2
Hard	O	531.3	11.7
		532.4	3.4
		534.3	2.5
	N	399.7	3.3
	C	284.6	57.6
		286.5	14.7
		288.3	6.8

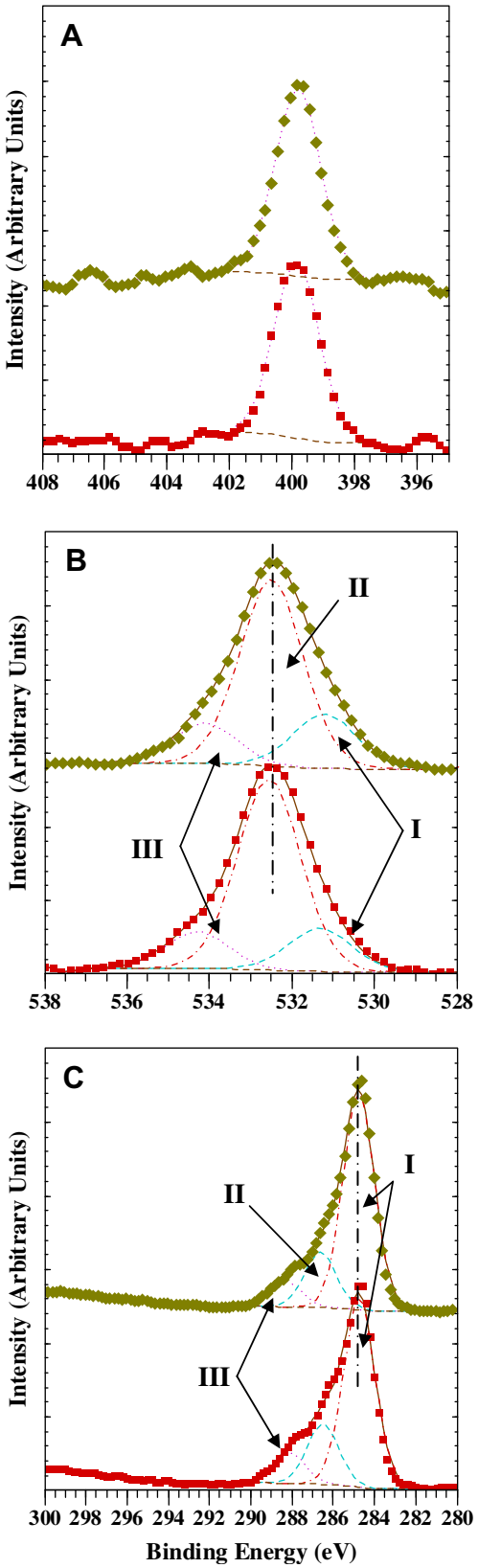

Fig. 4. XPS spectra obtained on near-isogenic soft and hard wheat flours. (A) nitrogen (N 1*s*); single peak at BE = 399.8 eV. (B) oxygen (O 1*s*); the main peak is deconvoluted with three distinct peaks labeled I, II and III. (C) carbon (C 1*s*); the spectra can be deconvoluted with three distinct peaks labeled I, II and III.

spectra of O 1*s* and C 1*s* can be deconvoluted with three peaks. Fig. 4B shows the O 1*s* spectra in which the three peaks are labeled I, II and III. The energy position of these peaks is 531.3, 532.5 and 534.3 eV, respectively. The peaks are assigned, (1) to oxygen doubly bonded to carbon, due to carboxyl and ester (peak I), (2) to oxygen making single bonds with carbon (peak II), and (3) to oxygen singly bonded to carbon (peak III). Fig. 4C displays the XPS spectra of C 1s. Three deconvoluted peaks labeled I, II and III are attributed to C–(C, H) at BE ~ 284.7 eV (I), to C–(O, N) at about 286.5 eV (II) and to C–C–O or C=O for the peak at ~288.2 eV (III). The concentration of proteins can be estimated by the ratio oxygen/carbon. The calculated ratios O/C for soft and hard wheat flours are 0.26 and 0.22, respectively. The assignments for C, O and N and the ratio O/C are in relatively good agreement with the work done by Rouxhet et al. (2008). The estimated ratios O to N are 6.6 and 5.3, respectively. These ratios (O/C and O/N) are rough estimates because a more detailed calculation of carbohydrate (C–O) and peptide (N–C=O) contributions is not possible due to the fact that carbon and oxygen are involved in several possible chemical species. Dumas elemental nitrogen content of these two flours was equal at 2.0% (9.7% protein on a 14% moisture basis). In conclusion, XPS measurements provided some insight into the chemical concentration of the different species constituting wheat flours but an accurate quantification of protein and carbohydrate in these complex systems (wheat flour) is not possible with this technique.

The four techniques used in this work have unique inherent limitations. They were utilized to assess differences between kernel types. Each technique provides different information. SEM uses an energetic electron beam that could generate very high resolution images. However, charging effect (brighter lines/features as seen in Fig 1) if not neutralized (by coating the surface with carbon or gold) can often make high resolution imaging impossible. Larger-scale images (a few mm) are easily obtained (Fig. 1A and B) and difference in microstructure quickly assessed (Fig. 1C–F). In contrast, AFM imaging is possible on any flat surfaces independent of the type of material (insulator or conductor) from the micron to nanometer scale. However, rough surfaces (>5 μm) are impossible to image due to the scanner limited travelling distance often requiring the polishing of the surface. On the other hand, AFM allows topographic information of a surface (e.g. average roughness, particle and pore analysis, height, diameter and area distributions and the display of 3D images) which is not possible with SEM. We report in this contribution the average roughness of the surface and surface area ratio obtained with the AFM. Raman provides chemical information such as vibrational bands (functional groups) and vibrational modes (summarized in Table 1) and frequencies which is not possible with XPS. Raman spectroscopy allows quantitative information by using the relative intensities of the bands to assess for instance the arabino-to-xylan substitution and the phenolic acid contents, as done in this work (Fig. 3) and by Barton and Himmelsbach (2002). On the other hand, XPS analysis yields surface relative chemical composition (detected elements) and chemical bonding information of these elements as seen in Fig. 4B and C and summarized in Table 2 which is not possible with Raman, SEM and AFM. In summary, based on their own specificity, these four techniques identified differences between soft and hard wheat kernels that could be used as starting points towards a better understanding of this important phenomenon.

4. Conclusion

In this contribution we have used four different techniques to image and probe soft and hard wheat kernel endosperms and their corresponding roller milled flours. Secondary field emission scanning electron microscopy (FE SEM) revealed microstructure

differences between interior polished soft and hard wheat endosperms. Atomic force microscopy (AFM) images also identified different morphological and topographical features between soft and hard kernels. The hard kernel exhibited a more granular texture consisting of distinct spheroid features (10–50 nm in diameter), while granular clustering was observed in the soft kernel endosperm. The hard kernel showed a higher surface ratio (surface area/scanning area) than the soft kernel indicating a denser endosperm that could be related to the fundamental differences between adhesion/microscopic structure and composition between the kernels. Raman spectroscopy showed several distinct but similar bands for both flours. However, the intensity and relative intensity ratios of the bands were different for soft compared to hard wheat flour. This result could be used to access arabinoxylan and/or phenolic acid contents in the two types of flour. Finally, X-ray photoelectron spectroscopy, XPS, showed that the carbon and oxygen peaks can be deconvoluted into three chemical species and that the concentration of carbon, oxygen and nitrogen were slightly different between soft and hard wheat flour. Although the primary difference between soft and hard kernel endosperm texture still awaits a full explanation, the present work contributes to the ongoing research aimed to understand this important phenomenon.

Acknowledgements

The assistance of Valerie Lynch-Holm and the Washington State Univ. Franceshi Microscopy & Imaging Center is gratefully acknowledged. G. E. King and the staff of the Western Wheat Quality Lab produced the kernel and flour samples used here, along with the protein analyses. Stacey Sykes and Shawna Vogl contributed to the production of the manuscript and figures.

Supplementary data

Supplementary data associated with this article can be found in the online version, at doi:10.1016/j.jcs.2010.04.005.

References

Alizadeh-Pasdar, N., Nakai, S., Li-Chan, E.C.Y., 2002. Principal component similarity analysis of Raman spectra to study the effects of pH, heating, and *k*-Carrageenan on whey protein structure. Journal of Agricultural and Food Chemistry 50, 6042–6052.

Arboleda, P.H., Loppnow, G.R., 2000. Raman spectroscopy as a discovery tool in carbohydrate chemistry. Analytical Chemistry 72, 2093–2098.

Baker, A.A., Miles, M.J., Helbert, W., 2001. Internal structure of the starch granule revealed by AFM. Carbohydrate Research 330, 249–256.

Baranska, M., Schulz, H., Baranski, R., Nothnagel, T., Christensen, L.P., 2005. In situ simultaneous analysis of polyacetylenes, carotenoids and polysaccharides in carrot roots. Journal of Agricultural and Food Chemistry 53, 6565–6571.

Barron, C., Rouau, X., 2008. FTIR and Raman signatures of wheat grain peripheral tissues. Cereal Chemistry 85, 619–625.

Barton II, F.E., Himmelsbach, D.S., 2002. Applications of vibrational spectroscopy to the analysis and study of forages. In: Chalmers, J., Griffiths, P. (Eds.), Handbook of Vibrational Spectroscopy, vol. 5. Wiley & Sons, New York, pp. 3683–3692.

Bhave, M., Morris, C.F., 2008a. Molecular genetics of puroindolines and related genes: allelic diversity in wheat and other grasses. Plant Molecular Biology 66, 205–219.

Bhave, M., Morris, C.F., 2008b. Molecular genetics of puroindolines and related genes: regulation of expression, membrane binding properties and applications. Plant Molecular Biology 66, 221–231.

Binnig, G., Quate, C.F., Gerber, C., 1986. Atomic force microscope. Physical Review Letters 56, 930–933.

Bolshakova, A.V., Kiselyova, O.I., Yaminsky, I.V., 2004. Microbial surfaces investigated using atomic force microscopy. Biotechnology Progress 20, 1615–1622.

Bulkin, B.J., Kwak, Y., Dea, I.C.M., 1987. Retrogradation kinetics of waxy-corn and potato starches; a rapid, Raman-spectroscopic study. Carbohydrate Research 160, 95–112.

Cao, Y., Shen, D., Lu, Y., Huang, Y., 2006. A Raman-scattering study on the net orientation of biomacromolecules in the outer epidermal walls of mature wheat stems (*Triticum aestivum*). Annals of Botany 97, 1091–1094.

Celedon, A., Aguilera, J.M., 2002. Applications of microprobe Raman spectroscopy in food science. Food Science and Technology International 8, 101–108.

Centre for Advanced Microscopy (CfAM), 2006. MicroNote 108. University of Reading, Whiteknights, Reading, UK. http://www.reading.ac.uk/cfam/micronotes/index.htm.

Dhanasettakorn, K., 2008. Coenzyme Q10 content, composition, texture and physiochemical characteristics of pasta fortified with freeze-dried beef heart. University of Missouri-Columbia, Ph.D. thesis.

Dufrene, Y.F., 2001. Application of atomic force microscopy to microbial surfaces: from reconstituted cell surface layers to living cells. Micron 32, 153–165.

Fechner, P.M., Wartewig, S., Kleinebudde, P., Neubert, R.H.H., 2005. Studies of the retrogradation process for various starch gels using Raman spectroscopy. Carbohydrate Research 340, 2563–2568.

Howell, N.K., Arteaga, G., Nakai, S., Li-Chan, E.C.Y., 1999. Raman spectral analysis in the C–H stretching region of proteins and amino acids for investigation of hydrophobic interactions. Journal of Agricultural and Food Chemistry 47, 924–933.

Jeffers, H.C., Rubenthaler, G.L., 1977. Effect of roll temperature on flour yield with the Brabender Quadrumat experimental mills. Cereal Chemistry 54, 1018–1025.

Juszczak, L., Fortuna, T., Krok, F., 2003. Non-contact atomic force microscopy of starch granules surface. Part II. Selected cereal starches. Starch/Starke 55, 8–18.

Liu, Y., Chao, K., Kim, M.S., Tuschel, D., Olkhovyk, O., Priore, R.J., 2009. Potential of Raman spectroscopy and imaging methods for rapid and routine screening of the presence of melamine in animal feed and foods. Applied Spectroscopy 63, 477–480.

Meng, G., Chan, J.C.K., Rousseau, D., Li-Chan, E.C.Y., 2005. Study of protein–lipid interactions at the bovine serum albumin/oil interface by Raman microspectroscopy. Journal of Agricultural and Food Chemistry 53, 845–852.

Morris, C.F., 2002. Puroindolines: the molecular genetic basis of wheat grain hardness. Plant Molecular Biology 48, 633–647.

Morris, C.F., King, G.E., 2008. Registration of hard kernel puroindoline allele near-isogenic line hexaploid wheat genetic stocks. Journal of Plant Registrations 2, 67–68.

Morris, C.F., Pitts, M.J., Bettge, A.D., Pecka, K., McCluskey, P.J., 2008a. The compressive strength of wheat endosperm: Analysis of endosperm 'bricks'. Cereal Chemistry 85, 351–358.

Morris, C.F., Bettge, A.D., Pitts, M.J., King, G.E., Pecka, K., McCluskey, P.J., 2008b. The compressive strength of wheat endosperm: Comparison of endosperm 'bricks' to the single kernel characterization system. Cereal Chemistry 85, 359–365.

Morris, V.J., Mackie, A.R., Wilde, A.R., Kirby, P.J., Mills, A.R., Gunning, A.P., 2001. Atomic Force Microscopy as a tool for interpreting the rheology of food biopolymers at the molecular level. Food Science Technology 34, 3–10.

Neethirajan, S., Thomson, D.J., Jayas, D.S., White, N.D.G., 2008. Characterization of the surface morphology of durum wheat starch granules using atomic force microscopy. Microscopy Research and Technique 71, 125–132.

Ohtani, T., Yoshino, T., Hagiwara, S., Maekawa, T., 2000. High-resolution imaging of starch granule structure using atomic force microscopy. Starch/Starke 52, 150–153.

Osborne, B.G., 2001. Near-infrared spectroscopy in food analysis. In: Meyers, R.A. (Ed.), Encyclopedia of Analytical Chemistry. John Wiley & Sons Ltd, Chichester, pp. 1–14.

Piot, O., Autran, J.-C., Manfait, M., 2000. Spatial distribution of protein and phenolic constituents in wheat grain as probed by confocal Raman microspectroscopy. Journal of Cereal Science 32, 57–71.

Piot, O., Autran, J.-C., Manfait, M., 2001. Investigation by confocal Raman microspectroscopy of the molecular factors responsible for grain cohesion in the *triticum aestivum* bread wheat. Role of the cell walls in the starchy endosperm. Journal of Cereal Science 34, 191–205.

Ridout, M.J., Parker, M.L., Hedley, C.L., Bogracheva, T.Y., Morris, V.J., 2006. Atomic force microscopy of pea starch: granule architecture of the *rug3-a, rug4-b, rug 5*-a and *lam*-c mutants. Carbohydrate Polymers 65, 64–74.

Rouxhet, P.G., Misselyn-Bauduin, A.M., Ahimou, F., Genet, M.J., Adriaensen, Y., Desille, T., Bodson, P., Deroanne, C., 2008. XPS analysis of food products: toward chemical functions and molecular compounds. Surface and Interface Analysis 40, 718–724.

Sandras, F., Pezolet, M., Marion, D., Grauby-Heywang, C., 2009. Raman study of the puroindoline-a/Lysopamitoylphosphatidylcholine interaction in free standing black films. Langmiur 25, 8181–8186.

Strehle, K.R., Rosch, P., Berg, D., Schulz, H., Popp, J., 2006. Quality control of commercially available essential oils by means of Raman spectroscopy. Journal of Agricultural and Food Chemistry 54, 7020–7026.

Synytsya, A., Copikova, J., Matejka, P., Machovic, V., 2003. Fourier transform Raman and infrared spectroscopy of pectins. Carbohydrate Polymers 54, 97–106.

Yang, H., Feng, G., Li, Y., 2004. Investigating the roughness of peach during controlled atmosphere storage by atomic force microscopy. ASAE/CSAE Meeting Paper No. 046186. ASAE, St. Joseph, MI.

Yang, J., Shao, Z., 1995. Recent advances in biological atomic force microscopy. Micron 26, 35–49.